

Article

Energy Exploitation of High-Temperature Geothermal Sources in Volcanic Areas—a Possible ORC Application in Phlegraean Fields (Southern Italy)

Angelo Algieri

Department of Mechanical, Energy and Management Engineering, University of Calabria,
Via P. Bucci-Cubo 46C, 87036 Arcavacata di Rende, Cosenza, Italy; a.algieri@unical.it; Tel.: +39-984-494665

Received: 9 February 2018; Accepted: 6 March 2018; Published: 10 March 2018

Abstract: This work aims to investigate the energy performances of small-scale Organic Rankine Cycles (ORCs) for the exploitation of high temperature geothermal sources in volcanic areas. For this purpose, a thermodynamic model has been developed, and a parametric analysis has been performed that considers subcritical and transcritical configurations, and different organic fluids (isobutane, isopentane, and R245ca). The investigation illustrates the significant effect of the temperature at the entrance of the expander on the ORC behaviour and the rise in system effectiveness when the internal heat exchange (IHE) is adopted. As a possible application, the analysis has focused on the active volcanic area of Phlegraean Fields (Southern Italy) where high temperature geothermal reservoirs are available at shallow depths. The work demonstrates that ORC systems represent a very interesting option for exploiting geothermal sources and increasing the share of energy production from renewables. In particular, the investigation has been performed considering a 1 kg/s geothermal mass flow rate at 230 °C. The comparative analysis highlights that transcritical configurations with IHE guarantee the highest performance. Isopentane is suggested to maximise the ORC electric efficiency (17.7%), while R245ca offers the highest electric power (91.3 kW_{el}). The selected systems are able to fulfil a significant quota of the annual electric load of domestic users in the area.

Keywords: organic Rankine cycle; geothermal source; transcritical cycle; internal heat exchange; domestic application; electricity production; volcanic area

1. Introduction

The development and exploitation of renewable sources are today considered fundamental steps towards overcoming the energy “trilemma” of affordability, supply security, and environmental protection [1–3]. Furthermore, the positive influence of the renewable sources promotion on local development opportunities, employment prospects, and social cohesion is expected. For this purpose, different actions have been proposed in the last decades to support the exploitation of alternative energies and to reduce the adoption of fossil fuels and the consequent greenhouse gas emissions (i.e., Kyoto Protocol, Paris Climate Agreement, etc.) [4–6].

The most recent statistical data provided by the International Energy Agency (IEA) show that the worldwide gross inland consumption in 2015 was equal to 109,124 TWh, and the share from renewable sources was 11.6% [7]. In the European Union (EU-28), the 2015 gross inland consumption was 18,951 TWh with 16.7% from renewable energies, while the corresponding values in 2010 were 20,520 TWh and 12.9%, respectively [8]. The target of the EU-28 by 2020 is at least a share of 20% in gross final energy consumption, as defined by the 2009/28/EC Directive adopted by European Parliament and Council [9]. Specifically, the directive has defined national overall targets for the energy share from renewable sources in gross final consumption in 2020 and the indicative trajectories to meet mandatory objectives. Therefore, each EU-28 Member State has defined a National Renewable Energy

Action Plan (NREAP) and the measures that are necessary to satisfy the planned quota of energy from renewables in the electricity, heating and cooling, and transport sectors. In this context, the increase in energy efficiency and technological development are fundamental to fulfilling the objectives.

Eurostat data reveals that 11 Member States of EU-28 have already satisfied the 2020 national targets in 2015 [8]. Among the others, Italy reached the designed share as shown in Figure 1, in which the current trajectory of renewable energy sources is compared to the indicative and NREAP profiles [8,10,11]. In particular, renewables contribution to the Italian gross electricity generation in 2015 is equal to 109.7 TWh, which corresponds to about 39% of the total amount [11]. The value is significantly higher than the corresponding rate defined in the national action plan for 2015 (80.2 TWh), and it is also higher than the 2020 target (105.9 TWh). However, geothermal energy is the unique renewable source that does not guarantee the planned value (6.3 percentage points to reaching the established threshold) [8,10]. As a consequence, it is fundamental to increase geothermal exploitation, taking into account that the source is independent of climatic and seasonal conditions and guarantees a reliable programmability in energy production [12,13].

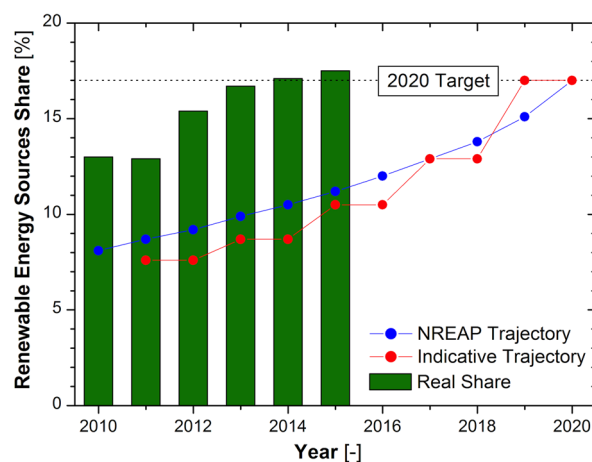


Figure 1. Italian renewable energy sources (RES) share: real, indicative, and NREAP trajectories.

The actual contribution of the heat beneath the surface of solid earth to the national electric production is limited to the Toscana region (Central Italy), even though high potential exists in the rest of the Italian peninsula and specific incentives are defined by the national legislation [14–16]. Furthermore, the exploitation of the active volcanic area represents a promising option due to the high temperature reservoirs' availability [17–21]. Nevertheless, few studies exist in the literature; for this reason, the present work focuses on the possible valorisation of geothermal sources in the active volcanic area of Phlegraean Fields Caldera (Southern Italy) by adopting small-scale Organic Rankine Cycle (ORC) units. Experimental campaigns performed by Agip and Enel, in fact, demonstrated the presence of high-enthalpy aquifers with temperatures higher than 200 °C at a very shallow depth [17,22,23]. In this framework, ORC is an attractive technology due to its high effectiveness, flexibility, and safety when compared with traditional energy systems for small-scale power applications and base load generation [24–27]. Furthermore, ORC requires low maintenance and guarantees fast start-up and stop procedures and efficient partial load operations [28,29]. The main differences between conventional and organic Rankine cycles lie in the adoption of an organic fluid, and the selection of the working fluid is essential to optimising system performances. To this purpose, the heat source temperature significantly influences the choice of the suitable fluids and the selection of the proper operating conditions [30–33]. It is worth noting that, nowadays, most geothermal installations present electric power higher than 200 kW_{el}, whereas few applications on small-scale ORCs are available due to higher investment costs and lower electric efficiencies [34], and further investigations are necessary to define proper configurations that are able to improve the global system efficiency.

To that end, a parametric analysis of small-scale units has been developed, and the influence of the operating conditions and ORC configuration on system behaviour has been estimated. Specifically, three organic fluids have been analysed and the effect of the internal regeneration has been investigated. Finally, results have been adopted to evaluate the possible use of geothermal-driven ORC to fulfill the electric request of domestic users in the volcanic area of Phlegraean Fields (Southern Italy).

2. Methodology

2.1. Thermodynamic Model

Organic Rankine Cycles (ORCs) consist mainly of a pump, an evaporator, a turbine/expander, and a condenser (Figure 2). The organic working fluid is compressed by a pump (1-2 process) then it is preheated (2-3) and vaporised (3-4) in the evaporator. The turbine expands the fluid to the condensing pressure (5-6) and, finally, a condensation takes place to obtain saturated liquid (6-1). An internal heat exchange (IHE) can be adopted to recover the thermal energy at the expander exit (6-7) and preheat the compressed liquid before the evaporation process occurs (2-9) in order to increase the effectiveness of the system. In geothermal applications, the heat beneath the earth's crust is used to provide the thermal energy to the organic fluid. Then, the geofluid is pumped to the heat exchanger from the geothermal reservoir and then reinjected into the ground. The corresponding processes in the T-s diagram for a typical dry organic fluid with subcritical and transcritical cycles are illustrated in Figure 3a,b, respectively. It is worth noting that the low critical pressure of organic fluids makes supercritical configurations very attractive without running into dangerous and extreme operating conditions.

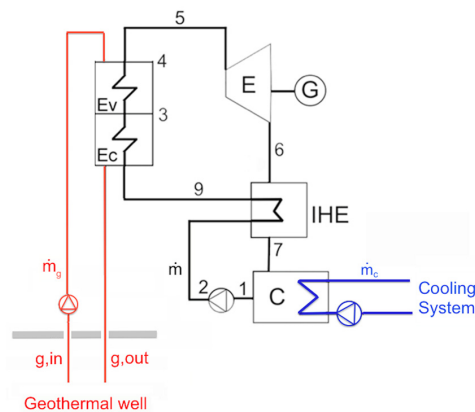


Figure 2. Scheme of geothermal Organic Rankine Cycle (ORC) system.

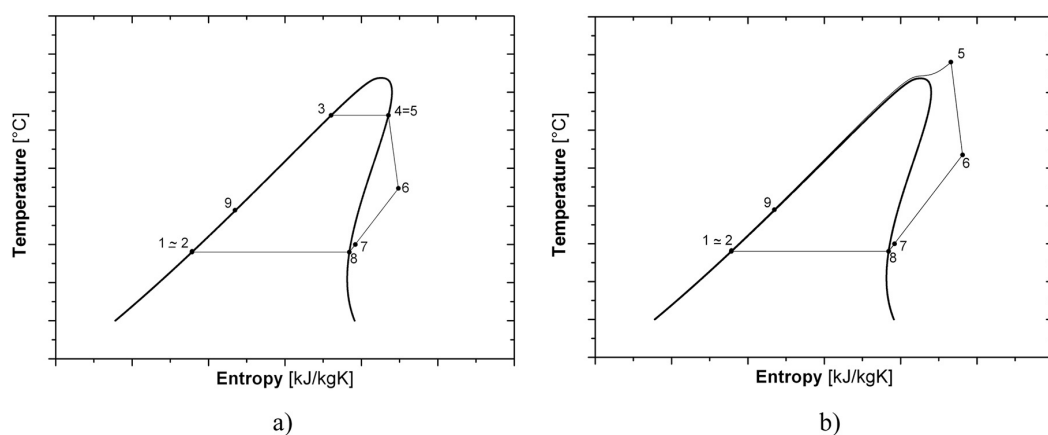


Figure 3. Subcritical (a) and transcritical (b) ORC cycle.

A thermodynamic model has been developed to evaluate the behaviour of geothermal ORCs [35–37]. The model has been coupled with the REFPROP database to define the properties of the working fluids [38]. A steady state condition has been assumed, whereas heat losses and pressure drops in system components have been neglected.

Thermal efficiency and net-specific work have been used as main indicators of the cycle performance. Specifically, the thermal efficiency η_{th} is defined as follows:

$$\eta_{th} = \frac{w}{q_i} \quad (1)$$

in which w is the specific work and q_i is the thermal heat transferred to the working fluid.

The net specific work represents the difference between the turbine and the pump work (w_t and w_p , respectively):

$$w = w_t - w_p = h_2 - h_1 + h_5 - h_6 \quad (2)$$

in which h_i represents the enthalpy of the working fluid in the generic state point i .

The heat transferred to the organic fluid q_i is

$$q_i = h_5 - h_2 \quad (3)$$

when the internal regenerator is absent, while

$$q_i = h_5 - h_9 \quad (4)$$

when the internal heat exchanger is adopted. According to the literature [26,28], the efficiency of the internal regenerator is defined as

$$\eta_{IHE} = \frac{h_9 - h_2}{h_6 - h_7} \quad (5)$$

2.2. Geothermal Source Exploitation

The analysis has focused on the Phlegraean Fields caldera area (Southern Italy) to evaluate the possible exploitation of high temperature geothermal sources for electric production. The area represents, in fact, a very interesting location for geothermal ORC systems owing to the abundant availability of geofluid reservoirs at relatively shallow depths. Drilling campaigns performed by Enel and Agip demonstrated the presence of high temperature aquifers. In particular, two productive reservoirs at less than 2000 m in depth are available in the Mofete area with water mass flow rates equal to 55 and 20 L/s and reservoir temperatures of 250 °C and 300 °C [17].

The performances of geothermal ORC systems have been characterised in terms of electric power and efficiency. The net electrical power P_{el} is

$$P_{el} = \eta_{em} P_t - P_p - P_{cp} \quad (6)$$

In particular, the efficiency η_{em} takes into account the generator electrical and mechanical losses; P_t is the turbine power, while P_p is the ORC pump power consumption, evaluated according to the following equations:

$$P_t = \dot{m} (h_5 - h_6) \quad (7)$$

$$P_p = \dot{m} (h_2 - h_1) \quad (8)$$

Furthermore, P_{cp} represents the power consumption of the circulating pump in the cooling system:

$$P_{cp} = \frac{\dot{m}_c g H_m}{\eta_{cp}} \quad (9)$$

in which g is the gravitational acceleration, H_m is the circulating pump head, η_{cp} represents the efficiency of the circulating pump, and \dot{m}_c is the mass flow rate of the cooling water.

The electric efficiency η_{el} of the ORC system is evaluated as

$$\eta_{el} = \frac{P_{el}}{\dot{Q}_{th}} \quad (10)$$

Specifically, the geothermal power \dot{Q}_{th} has been calculated as follows:

$$\dot{Q}_{th} = \dot{m}_g (h_{g,in} - h_{g,out}) \quad (11)$$

in which:

\dot{m}_g is the mass flow rate of the geothermal water;

h_g is the enthalpy of the geothermal water at the inlet (*in*) and outlet (*out*) section of the heat exchanger.

It has been assumed that the thermal power is transmitted from the geothermal water to the organic fluid within a heat exchanger, whose efficiency is η_{he}

$$\dot{Q}_i = \dot{m} q_i = \eta_{he} \dot{Q}_{th} \quad (12)$$

The model has been validated adopting literature data and shows an optimal agreement. As an example, the model reproduced the results of Liu et al. [39] registered for saturated configurations with percentage differences always lower than 2%.

2.3. Operating Conditions

For the investigation of the ORC performance, isobutane, isopentane, and R245ca have been adopted as organic working fluid, owing to their properties, consistent with geothermal sources [40–42]. Subcritical and transcritical cycles have been analysed by adopting saturated and superheated conditions at the entrance of the expander. Table 1 summarises the critical pressures and temperatures of the selected organic fluids and the operating conditions used during the investigation. In particular, the condensation temperature has always been set to 30 °C. For subcritical configurations, the evaporation temperature ranges between 70 °C and a maximum value that depends on the investigated fluid. Specifically, for isobutane, the maximum evaporation temperature is limited to 109 °C, while the corresponding maximum values are 149 °C and 172 °C for R245ca and isopentane, respectively, to avoid the presence of liquid during the expansion phase. For transcritical cycles, the maximum pressure has been imposed equal to 1.03 p_{crit} as suggested in the literature [43], while the maximum temperature is restricted to 220 °C.

Main assumptions adopted for the investigation are summarised in Table 2. According to the literature, the ORC turbine and pump effectiveness have been fixed to 70% and 60%, respectively; the effectiveness of the internal regenerator has been set to 95%; the efficiency of the heating process (from the geothermal water to the organic fluid) is 90%; and the electro-mechanical efficiency is 95%, while the temperature of the vapour at the internal regenerator outlet (T_7) has been assumed to be 10 °C higher than the condensation temperature [28,44]. For the circulating pump in the cooling system, head and efficiency have been set equal to 10 m and 80%, whereas the pinch point temperature in the cooling system is fixed at 5 °C [39,45]. The minimum reinjection temperature of the geothermal water ($T_{g,out}$) has been set at 70 °C to avoid fouling and scaling phenomena within pipes and system components, as suggested in the literature [24,39]. The reference minimum pinch-point temperature is 10 °C. The value has to be increased when the requirement on the minimum reinjection temperature is not satisfied. The performances of ORC systems have been characterised considering a 1 kg/s of geothermal water at 230 °C.

Table 1. Critical conditions of selected organic fluids and ORC operating conditions.

		Isobutane	Isopentane	R245ca
Critical conditions				
Critical temperature	[°C]	134.66	187.2	174.42
Critical pressure	[bar]	36.29	33.78	39.25
Subcritical cycles				
Condensation temperature	[°C]	30	30	30
Condensation pressure	[bar]	4.05	1.09	1.22
Evaporation temperature	[°C]	70–109	70–172	70–149
Evaporation pressure	[bar]	10.87–21.78	3.56–26.70	4.36–25.13
Transcritical cycles				
Condensation temperature	[°C]	30	30	30
Condensation pressure	[bar]	4.05	1.09	1.22
Maximum temperature	[°C]	140–220	195–220	180–220
Maximum pressure	[bar]	37.38	34.79	40.43

Table 2. Main assumption for the energy investigation.

Parameters	Units	Values
Expander efficiency	[%]	70
Pump efficiency	[%]	60
Internal heat exchanger efficiency	[%]	95
Internal heat exchanger temperature difference	[°C]	10
Boiler and geothermal circuit efficiency	[%]	90
Electro-mechanical efficiency	[%]	95
Cooling pump efficiency	[%]	80
Head of cooling pump	[m]	10
Pinch-point temperature in cooling system	[°C]	5
Minimum reinjection temperature	[°C]	70
Pinch-point temperature in geothermal circuit	[°C]	10
Mass flow rate of geothermal fluid	[kg/s]	1
Temperature of geothermal fluid	[°C]	230

3. Results and Discussion

A parametric analysis on the energetic performances of Organic Rankine Cycles (ORCs) for the exploitation of geothermal sources has been carried out. To this purpose, isobutane, isopentane, and R245ca have been adopted as working fluids, and the influence of the ORC configurations and operating conditions on the system behaviour has been investigated. Specifically, subcritical and transcritical cycles have been compared, and the effect of the internal regenerator has been evaluated.

Figure 4a illustrates the thermal efficiency of subcritical systems when saturated conditions at the entrance of the expander are adopted. The analysis refers to a condensation temperature equal to 30 °C. Minimum evaporation temperature has been fixed to 70 °C, whereas the maximum value has been defined to prevent the presence of liquid during the expansion process, and it depends on the organic fluid characteristics and slope of the saturated vapour curve.

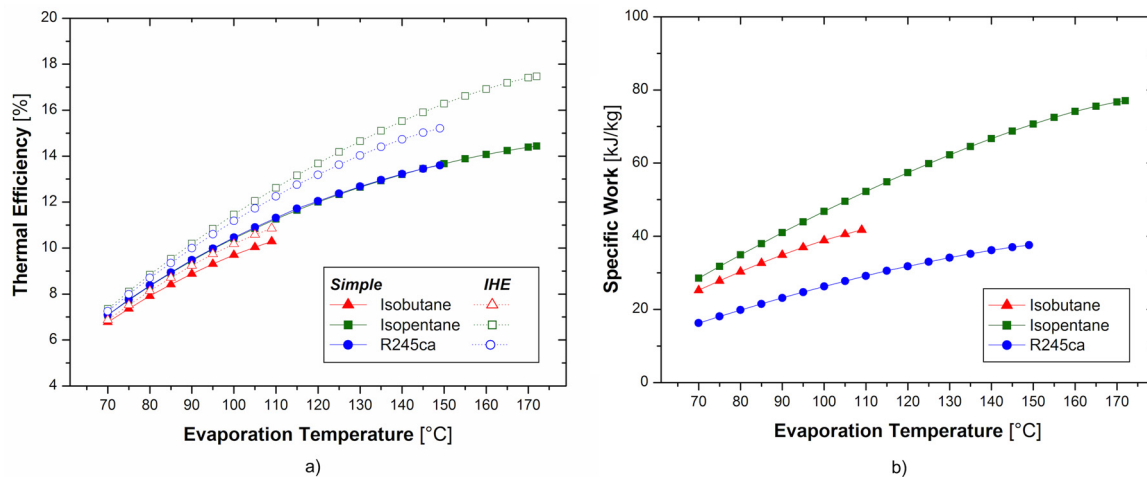


Figure 4. Influence of evaporation temperature on ORC efficiency (a) and specific work (b) (subcritical cycle).

Results show a progressive upsurge in the ORC effectiveness with the evaporation temperature according to the literature [26,46]. Furthermore, a positive influence of the internal heat exchange (IHE) is noticed. The highest cycle efficiency (17.5%), in fact, is found by adopting regenerative systems with isopentane at 172 °C, whereas the corresponding maximum values for R245ca and isobutane are 15.2% (at 149 °C) and 10.9% (at 109 °C), respectively. The effect of internal regeneration reduces when the evaporation temperature decreases. Particularly, the absolute rise in the system efficiency moving from simple to IHE configurations is always lower than 1% when the evaporation temperature is below 95 °C. In these conditions, results suggest that it would be best to adopt the simple configuration without internal regenerator due to the higher system simplicity and lower cost.

When the simple configuration is considered, isopentane and R245ca offer similar efficiencies, while isobutane presents lower performance for all the investigated evaporation temperatures. Values larger than 6.7% are always registered at 70 °C, and the thermal efficiency is higher than 10% when the evaporation temperature is higher than 105 °C.

The evaporation temperature also has a positive influence on the specific work, with a continuous increase in the thermal level (Figure 4b). Differences between the three investigated fluids upsurge with the evaporation temperature, and significant differences exist, although similar cycle efficiencies have been registered. At 70 °C, isopentane presents a net specific work equal to 28.6 kJ/kg, whereas the corresponding value reduces to 25.2 and 16.3 kJ/kg when isobutane and R245ca are used, respectively. At 100 °C, the net specific work ranges between 26.3 kJ/kg (R245ca) and 46.8 kJ/kg (isopentane). The maximum value (77.0 kJ/kg) is found with isopentane at 172 °C. The analysis reveals that the pump work is always lower than 7.0 kJ/kg for all the investigated configurations and ranges from 2.3% (isopentane at 70 °C) to 12.4% (isobutane at 109 °C) of the expander work. The internal regeneration does not affect the ORC specific work.

The analysis has been extended to transcritical configurations with superheated conditions at the inlet of the expander. The maximum pressure has been set to $1.03 p_{crit}$, as suggested in the literature [43]. The condensation temperature is always 30 °C, while the maximum thermal level has been fixed at 220 °C. The influence of the expander inlet temperature on the cycle effectiveness is negligible if the simple configuration is adopted. Specifically, the efficiency maintains near 12% for isobutane and 15% for R245ca and isopentane (Figure 5a).

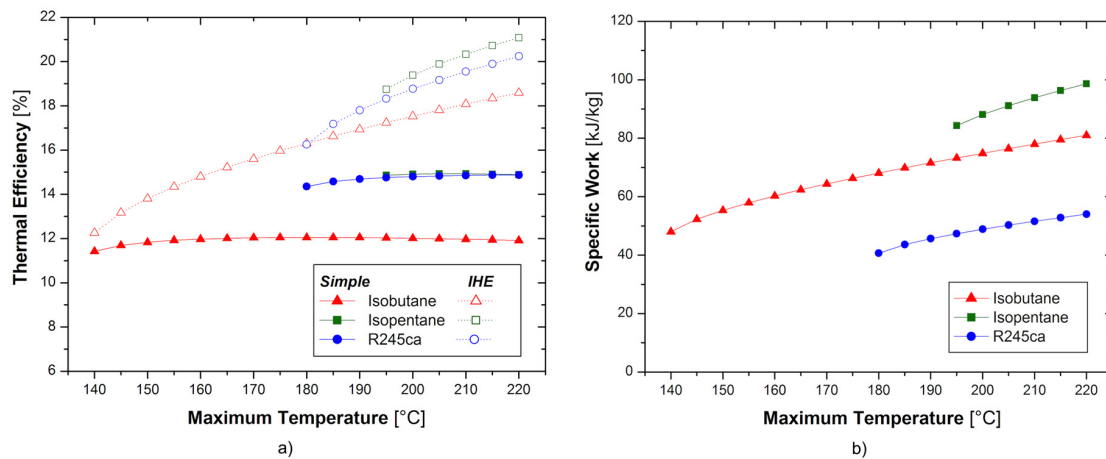


Figure 5. Effect of maximum temperature on ORC efficiency (a) and specific work (b) (transcritical cycle).

On the other hand, the maximum temperature has a noticeable impact on regenerative units: the higher the thermal level, the higher the system performance. As already observed for subcritical configurations, isopentane exhibits better results. Particularly, the maximum ORC effectiveness reaches 21.1% at 220 °C, with a 41.6% increase with respect to the corresponding value obtained for the simple cycle, and all the IHE configurations exhibit efficiencies higher than 16% when the maximum temperature is higher than 180 °C. Figure 5b highlights that the rise in the energy content of the organic fluid also has a positive influence on the net specific work due to the progressive increase in the turbine output, while the pump energy request is independent from the maximum operating temperature. At 200 °C the specific work ranges between 48.9 kJ/kg (R245ca) and 88.0 kJ/kg (isopentane), and it reaches 54.0 and 98.6 kJ/kg at 220 °C, respectively.

A Possible ORC Domestic Application in the Phlegraean Fields Area

As a possible application, the exploitation of geothermal sources in ORC systems has been analysed while considering the volcanic area of Phlegraean Fields caldera, where different geothermal wells are present; furthermore, an interesting potential for small-scale applications exists [17,22,23]. The area is located in the Campania Region (Southern Italy) and covers about 8000 hectares (Figure 6).



Figure 6. Investigated area: Phlegraean Fields (Campania Region—Southern Italy).

Figure 7 depicts the potential electric power of saturated ORC units when the mass flow rate and temperature of the geothermal fluid are 1 kg/s and 230 °C, respectively. Results confirm the progressive increase in the system performances with the evaporation temperature and the positive influence of the internal heat exchange. Specifically, isopentane guarantees the highest level of electric power ($P_{el} = 89.7 \text{ kW}_{el}$ at $T_e = 220 \text{ °C}$ with internal regenerator), while negligible differences between the different configurations and organic fluids are observed at low thermal levels ($P_{el} \approx 35 \text{ kW}_{el}$).

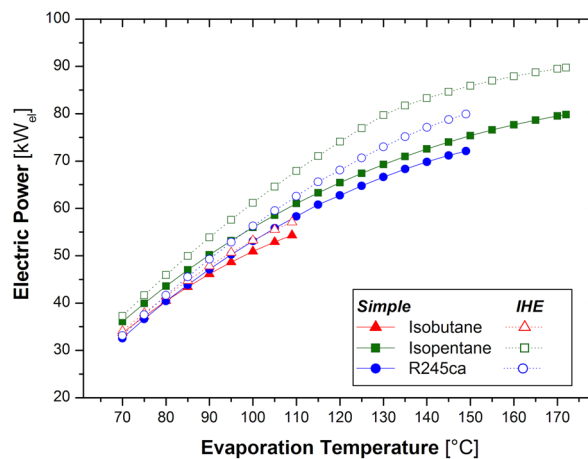


Figure 7. Effect of evaporation temperature on ORC electric power (subcritical cycle).

The plot shows a change in the slope of the curve corresponding to the system with IHE and isopentane, owing to the variation in the reinjection temperature and, as a consequence, in the thermal input to ORC units (Figure 8a). In fact, the minimum reinjection temperature has been set equal to 70 °C to avoid scaling and fouling problems in heat exchangers and pipes, as suggested in the literature, and this value is registered for all the saturated configurations except for the regenerative system with isopentane and evaporation temperatures higher than 130 °C. In these cases, the high thermal level of the organic fluid at the entrance of the economiser IHE and the minimum pinch-point temperature (10 °C) determines reinjection temperatures larger than the minimum value.

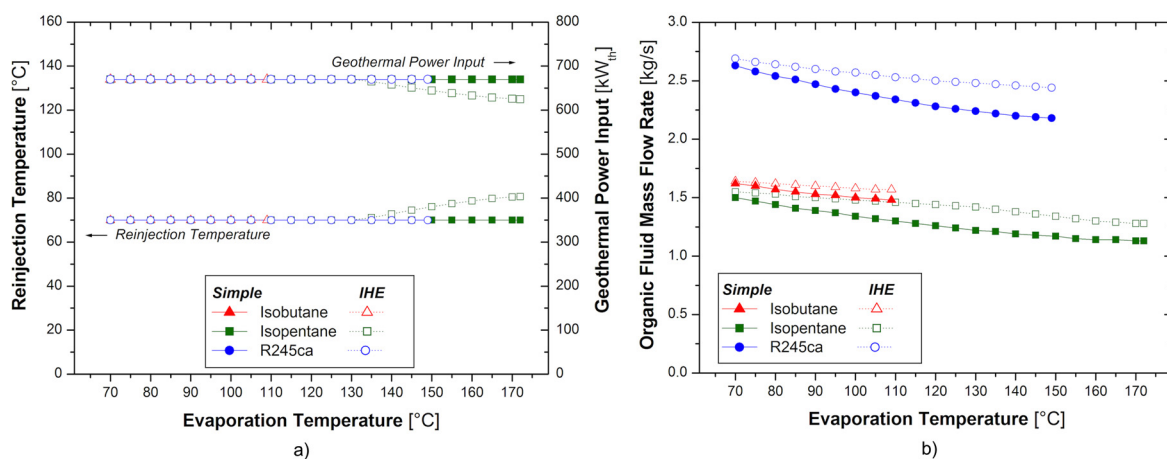


Figure 8. Influence of evaporation temperature on geothermal reinjection temperature and power input (a). Effect of the evaporation temperature on organic mass flow rate (b). Saturated cycle.

The influence of the evaporation level on the organic fluid mass flow rate is shown in Figure 8b. A progressive decrease is evident when the temperature at the expander inlet rises, whereas the internal heat exchanger guarantees slightly higher mass flow with respect to the simple arrangement.

Isobutane and isopentane exhibit similar values, in the range between 1.1 and 1.6 kg/s, while mass flows higher than 2 kg/s are registered for R245ca.

A different behaviour in ORC electric power is registered for transcritical systems (Figure 9a). Isobutane and R245ca curves present a maximum, while a continuous decrease is noticed for isopentane when the temperature at the expander inlet increases, despite the progressive rise in the electric efficiency observed for all the investigated configurations, as shown in Figure 9b. R245ca guarantees the highest electric power ($P_{el} = 91.3 \text{ kW}_{el}$) when the internal regeneration is adopted and the temperature at the expander entrance is equal to 185 °C. For the simple configuration the maximum is located at 195 °C, and the same values of the IHE arrangement are found when the temperature is larger than 200 °C.

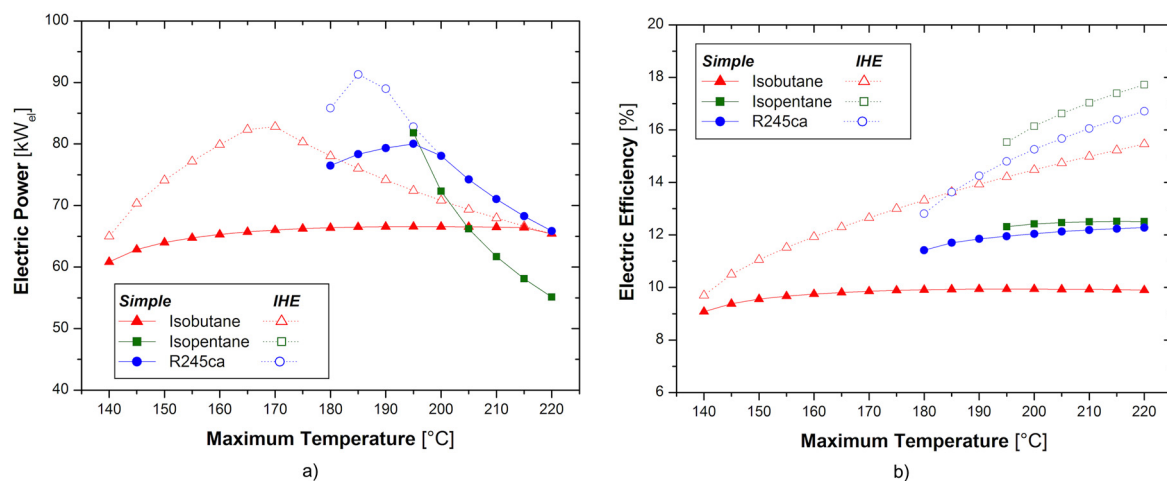


Figure 9. Effect of maximum temperature on ORC electric power (a) and electric efficiency (b) (transcritical cycle).

A similar trend is noticed for isobutane, and the peak in the electric power is 82.8 kW_{el} at 170 °C. Simple and IHE results overlap for $T_{max} > 215$ °C. Isopentane offers the same electric power when the maximum temperature is fixed, independent from the presence of the internal regeneration.

The overlap between simple and IHE configurations is due to the balance between ORC electric efficiency and thermal input when the mass flow rate and the temperature of the geothermal source are defined. The adoption of the internal heat exchanger, in fact, permits improvement of the global effectiveness of the devices. At the same time, the reinjection temperature upsurges (Figure 10a) and, as a consequence, the thermal power from the geothermal water and the mass flow rate of working fluid (Figure 10b) reduce, according to Equations (11) and (12). Specifically, the difference between reinjection temperatures of IHE and simple cycles is larger than 30 °C when the maximum temperature of the organic fluid is higher than 200 °C and the difference is higher than 56 °C with isobutane at the maximum operating temperatures.

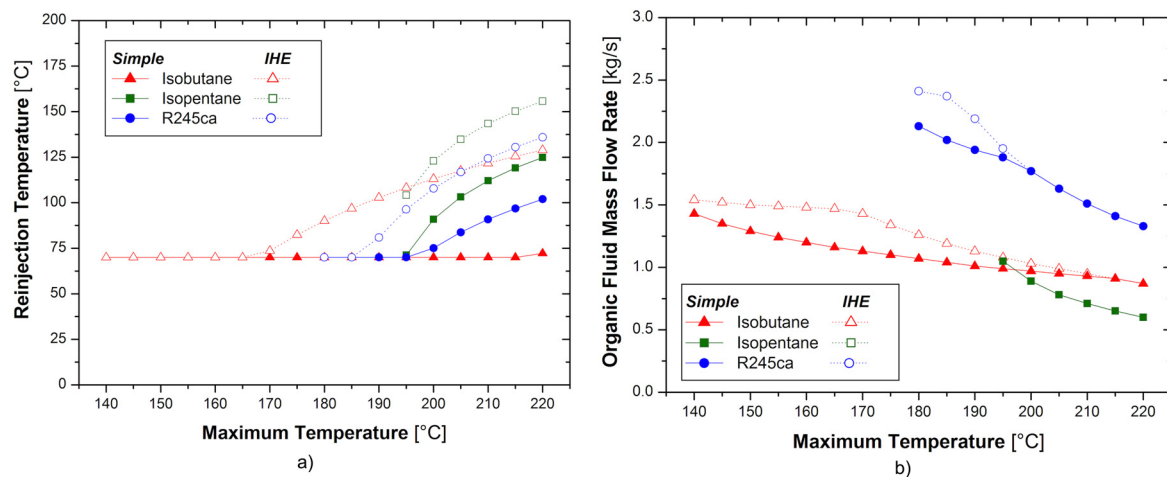


Figure 10. Effect of maximum temperature on geothermal reinjection temperature (a) and mass flow rate of organic fluid (b) (transcritical cycle).

It is noteworthy to observe that the increase in the reinjection temperature has a positive effect on the perturbations that the exploitation of the geothermal source generates, reducing pressure and thermal gradients and the induced risk seismicity due to the extraction and injection of geothermal fluids into reservoirs [17]. The analysis of the possible environmental impact of the geothermal valorisation is fundamental to guaranteeing a proper and sustainable development of this renewable source [12,47–49], especially in volcanic/seismic areas with a high-density population, as Phlegraean Fields Caldera is—but this issue is beyond the purpose of this work.

The comparison between subcritical and transcritical systems demonstrates that the latter configuration guarantees better results both in terms of efficiency and environmental perturbations, and the adoption of the internal regeneration improves systems performance. To this end, Table 3 summarises the ORC configurations that offer the highest electric power and the maximum electric efficiency. Specifically, when the temperature and the mass flow rate of the geothermal source are defined, data suggest adopting R245ca as the proper working fluid to maximise the electric power ($P_{el} = 91.3 \text{ kW}_{el}$, $\eta_{el} = 13.6\%$), while isopentane is recommended to obtain the highest electric effectiveness ($\eta_{el} = 17.7\%$ with $P_{el} = 55.1 \text{ kW}_{el}$).

Table 3. Main performances of selected ORC systems.

Operating Conditions	Units	Maximum Power	Maximum Efficiency
Cycle		Transcritical	Transcritical
System configuration		With IHE	With IHE
Working fluid		R245ca	Isopentane
Condensation temperature	[°C]	30.0	30.0
Condensation pressure	[bar]	1.22	1.09
Maximum temperature	[°C]	185.0	220.0
Maximum pressure	[bar]	40.43	34.79
Electric power	[kW _{el}]	91.3	55.1
Electric efficiency	[%]	13.6	17.7
Organic mass flow rate	[kg/s]	2.37	0.60
Reinjection temperature	[°C]	70.0	155.7

In particular, the more efficient unit has been selected to evaluate the possible adoption of ORC systems to satisfy the electric request of some domestic users in the investigated geographical area, due to its lower environmental impact due to the high reinjection temperature (155.7 °C), as already observed. Furthermore, the system is characterised by lower maximum pressure and mass flow rate.

Typical daily electric loads per apartment in winter, summer, and intermediate seasons in the region are shown in Figure 11, which consider the lighting system and electric appliance requests, including air conditioners, during the hot period [50].

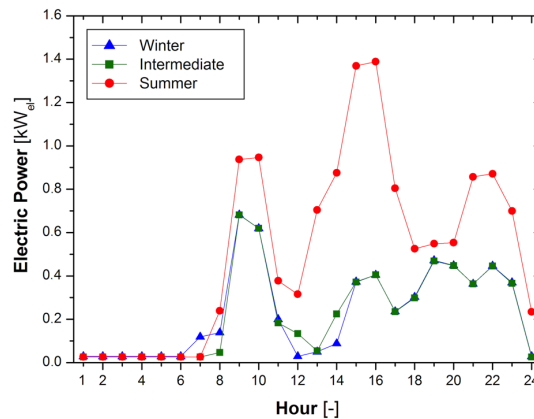


Figure 11. Typical electric load profiles for a single apartment in the investigated area during winter, intermediate, and summer season.

The maximum rectangle method has been adopted to define the number of dwellings that can be served by the selected ORC system [51]. The technique is based on the load-duration diagram and defines the proper size of the generation apparatus as the power that maximises the area of the rectangle that can be drawn below the load-duration curve. In this way, the generation system is used to fulfill an average electric request, while peak loads are satisfied by grid integration.

The analysis highlights that the system with the highest electric efficiency is able to fulfill 152 apartments, providing 277.0 MWh, which corresponds to 68.6% of the yearly electric load (404.0 MWh). The percentage reduces to 48.7% during the summer but is always higher than 83% during the rest of the year. At the same time, the electric energy injected into the grid is equal to 205.7 MWh, that is, 42.6% of the ORC energy production on a yearly basis, with a lower percentage registered during the hot season (30.5% corresponding to 37.1 MWh). Specifically, the daily energy balances for winter and summer term are highlighted in Figure 12. It is evident that a withdrawal from the grid is present when the electric request is higher than the energy production, while the energy in excess is injected into the network, especially during night hours.

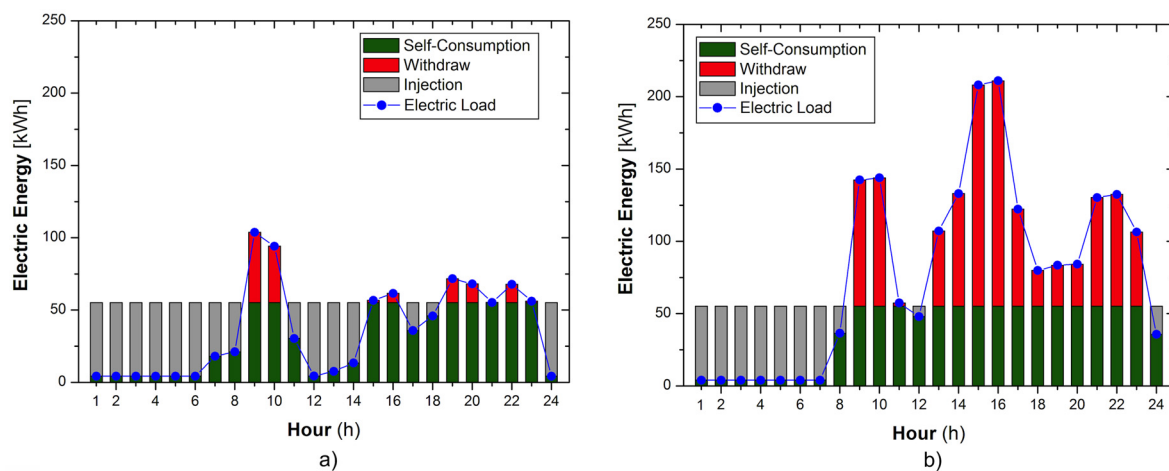


Figure 12. Hourly electric balance in winter (a) and summer (b) typical days. ORC electric production (self-consumption and electricity injected into the grid) and electric request of domestic users (with integration from the grid).

If the production excess has to be reduced, a threshold on the domestic load can be defined to switch on or switch off the ORC unit. As an example, Figure 13 depicts the daily balance when the threshold is fixed at 20% of the ORC nominal power. It is evident that when the electric request is lower than the ORC threshold, the unit is turned off and integration from the grid is necessary.

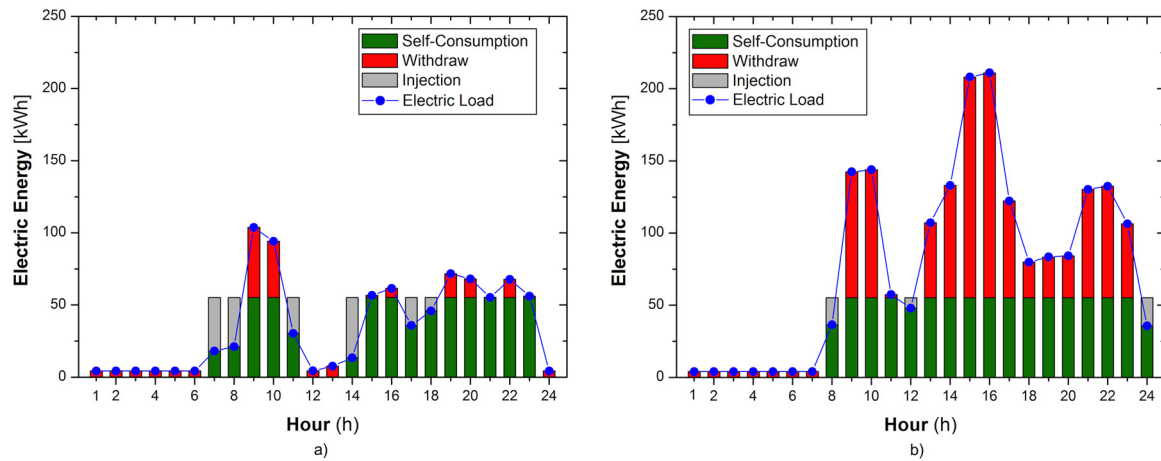


Figure 13. Hourly electric balance in winter (a) and summer (b) typical days. ORC electric production (self-consumption and electricity injected into the grid) and electric request of domestic users (with integration from the grid). ORC switch-off at 20% of nominal power.

In this case, 86.9% of the ORC yearly electric production is used for the 152 apartments, but the energy percentage from the grid rises to 35.1% of the domestic load. The influence of the threshold level on the electric balance is shown in Figure 14. The higher the starting value, the higher the withdrawal energy from the network and the lower the electric production.

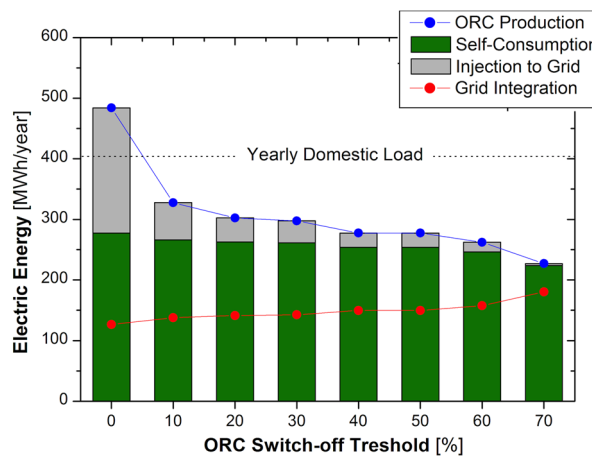


Figure 14. Influence of the ORC switch-off value on the yearly electric balance. ORC production (self-consumption and injection quota) and grid integration.

Similar results are found if the ORC with the highest electric power is used. In this case the system is able to satisfy the electric request of 251 apartments, but a lower reinjection temperature is obtained (70 °C) with higher environmental perturbations and seismic risk. The electricity balance maintains the same percentage values observed for the more efficient apparatus. In particular, the yearly ORC electric production is equal to 800.0 MWh, with 341.3 MWh injected to the grid and integration equal to 208.5 MWh when the threshold is not defined.

4. Conclusions

The present work has investigated the energetic performances of Organic Rankine Cycles (ORCs) for the exploitation of high temperature geothermal sources. To this purpose, subcritical and transcritical configurations have been considered, and the effect of the internal heat exchange (IHE) on the characteristics of the system has been evaluated by adopting three organic fluids (isobutane, isopentane, and R45ca).

The investigation demonstrates the relevant influence of the expander inlet temperature and the noticeable impact of the internal heat exchange on ORC thermal efficiency and specific work both in subcritical and transcritical cycles. In particular, the comparison between the investigated cycles highlights the fact that transcritical configurations with IHE guarantee the best results, and that system performances improve with the upsurge in the expander entrance thermal level. The maximum is registered when isopentane is selected as a working fluid and the temperature at the expander entrance is set to 220 °C. In this condition, the cycle efficiency reaches 21.1%, and the specific work is about 100 kJ/kg.

The exploitation of geothermal sources in ORC systems has been analysed while considering the active volcanic area of Phlegraean Fields Caldera (Southern Italy), where high temperature geothermal wells are present. The parametric analysis demonstrates that ORC systems appear to be a very interesting solution for small-scale geothermal applications in volcanic areas. In particular, when the flow rate and temperature of the geofluid are 1 kg/s and 230 °C, respectively, a net electric power higher than 33 kW_{el} is found for all the investigated units. The comparison between subcritical and transcritical systems demonstrates that the latter configuration guarantees better results and the adoption of the internal regeneration improves the system performance. Specifically, data suggest adopting R245ca as the proper working fluid and a maximum temperature at the expander inlet equal to 185 °C to maximise the electric power ($P_{el} = 91.3 \text{ kW}_{el}$), while isopentane at the highest thermal level ($T_{max} = 220 \text{ °C}$) is recommended to obtain the largest electric effectiveness ($\eta_{el} = 17.7\%$ with $P_{el} = 55.1 \text{ kW}_{el}$). In particular, the system with the highest electric efficiency is able to fulfill the electric request of 152 apartments, considering the typical daily profiles registered for the domestic sector in the Campania region. The value reaches 251 dwellings if the ORC unit with the highest electric power is considered. In both cases, ORC apparatus is able to provide more than 68% of the yearly electric load, with a maximum contribution during winter term (larger than 83%), while the annual electric energy injected to the grid is equal to 42.6%. It is worth noting that the more efficient ORC system permits the maintenance of higher reinjection temperatures, reducing the thermal gradient in the geothermal reservoirs due to the withdrawal and reinjection of the geothermal fluid, and the possible induced seismicity.

Conflicts of Interest: The author declares no conflict of interest.

References

1. Stempien, J.P.; Chan, S.H. Addressing energy trilemma via the modified Markowitz Mean-Variance Portfolio Optimization theory. *Appl. Energy* **2017**, *202*, 228–237. [CrossRef]
2. Qiu, G. Selection of working fluids for micro-CHP systems with ORC. *Renew. Energy* **2012**, *48*, 565–570. [CrossRef]
3. Qiu, G.; Shao, Y.; Li, J.; Liu, H.; Riffat, S.B. Experimental investigation of a biomass-fired ORC-based micro-CHP for domestic applications. *Fuel* **2012**, *96*, 374–382. [CrossRef]
4. United Nations. Kyoto Protocol to the United Nations Framework Convention on Climate Change. 1998. Available online: http://unfccc.int/kyoto_protocol/items/2830.php (accessed on 3 February 2018).

5. United Nations. Paris Agreement. 2015. Available online: http://unfccc.int/paris_agreement/items/9485.php (accessed on 3 February 2018).
6. Hong, Y.-Y.; Lai, Y.-M.; Chang, Y.-R.; Lee, Y.-D.; Liu, P.-W. Optimizing Capacities of Distributed Generation and Energy Storage in a Small Autonomous Power System Considering Uncertainty in Renewables. *Energies* **2015**, *8*, 2473–2492. [[CrossRef](#)]
7. International Energy Agency. Available online: <https://www.iea.org/statistics/> (accessed on 3 February 2018).
8. Eurostat. Available online: <http://ec.europa.eu/eurostat/web/energy/data> (accessed on 3 February 2018).
9. The European Parliament and the Council of the European Union. Directive 2009/28/EC of the European Parliament and of the Council. 2009. Available online: <http://eur-lex.europa.eu> (accessed on 3 February 2018).
10. Italian Ministry of Economic Development. Piano di Azione Nazionale per le Energie Rinnovabili (Direttiva 2009/28/CE). 2010. Available online: <http://unmig.mise.gov.it> (accessed on 3 February 2018).
11. European Commission—Joint Research Center. Available online: <http://iet.jrc.ec.europa.eu/remea/> (accessed on 3 February 2018).
12. Tomasini-Montenegro, C.; Santoyo-Castelazo, E.; Gujba, H.; Romero, R.J.; Santoyo, E. Life cycle assessment of geothermal power generation technologies: An updated review. *Appl. Therm. Eng.* **2017**, *114*, 1119–1136. [[CrossRef](#)]
13. Özkara, O.; Keçebaş, P.; Demircan, C.; Keçebaş, A. Thermodynamic Optimization of a Geothermal-Based Organic Rankine Cycle System Using an Artificial Bee Colony Algorithm. *Energies* **2017**, *10*, 1691. [[CrossRef](#)]
14. Terna. Available online: <http://www.terna.it/en-gb/sistemaelettrico.aspx> (accessed on 3 February 2018).
15. Italiano, F.; De Santis, A.; Favali, P.; Rainone, M.L.; Rusi, S.; Signanini, P. The Marsili Volcanic Seamount (Southern Tyrrhenian Sea): A Potential Offshore Geothermal Resource. *Energies* **2014**, *7*, 4068–4086. [[CrossRef](#)]
16. GSE. Available online: <https://www.gse.it/en> (accessed on 3 February 2018).
17. Carlino, S.; Troiano, A.; Di Giuseppe, M.G.; Tramelli, A.; Troise, C.; Somma, R.; De Natale, G. Exploitation of geothermal energy in active volcanic areas: A numerical modelling applied to high temperature Mofete geothermal field, at Campi Flegrei caldera (Southern Italy). *Renew. Energy* **2016**, *87*, 54–66. [[CrossRef](#)]
18. Cinti, D.; Procesi, M.; Poncia, P.P. Evaluation of the Theoretical Geothermal Potential of Inferred Geothermal Reservoirs within the Vicano–Cimino and the Sabatini Volcanic Districts (Central Italy) by the Application of the Volume Method. *Energies* **2018**, *11*, 142. [[CrossRef](#)]
19. Bertani, R. Geothermal power generation in the world 2010–2014 update report. *Geothermics* **2016**, *60*, 31–43. [[CrossRef](#)]
20. Paoletti, V.; Langella, G.; Di Napoli, R.; Amoresano, A.; Meo, S.; Pecoraino, G.; Aiuppa, A. A tool for evaluating geothermal power exploitability and its application to Ischia, Southern Italy. *Appl. Energy* **2015**, *139*, 303–312. [[CrossRef](#)]
21. Montanari, D.; Minissale, A.; Doveri, M.; Gola, G.; Trumpy, E.; Santilano, A.; Manzella, A. Geothermal resources within carbonate reservoirs in western Sicily (Italy): A review. *Earth-Sci. Rev.* **2017**, *169*, 180–201. [[CrossRef](#)]
22. Corrado, G.; De Lorenzo, S.; Mongelli, F.; Tramacere, A.; Zito, G. Surface heat flow density at the Phlegrean Fields caldera (Southern Italy). *Geothermics* **1998**, *27*, 469–484. [[CrossRef](#)]
23. Carlino, S.; Somma, R.; Troise, C.; De Natale, G. The geothermal exploration of Campanian volcanoes: Historical review and future development. *Renew. Sustain. Energy Rev.* **2012**, *16*, 1004–1030. [[CrossRef](#)]
24. Gao, T.; Liu, C. Off-Design Performances of Subcritical and Supercritical Organic Rankine Cycles in Geothermal Power Systems under an Optimal Control Strategy. *Energies* **2017**, *10*, 1185.
25. Wu, Z.; Pan, D.; Gao, N.; Zhu, T.; Xie, F. Experimental testing and numerical simulation of scroll expander in a small scale organic Rankine cycle system. *Appl. Therm. Eng.* **2015**, *87*, 529–537. [[CrossRef](#)]
26. Li, W.; Feng, X.; Yu, L.J.; Xu, J. Effects of evaporating temperature and internal heat exchanger on Organic Rankine Cycle. *Appl. Therm. Eng.* **2011**, *31*, 4014–4023. [[CrossRef](#)]
27. Saleh, B.; Koglbauer, G.; Wendland, M.; Fischer, J. Working fluids for low temperature Organic Rankine Cycles. *Energy* **2007**, *32*, 1210–1221. [[CrossRef](#)]

28. Drescher, U.; Bruggemann, D. Fluid selection for the Organic Rankine Cycle (ORC) in biomass power and heat plants. *Appl. Therm. Eng.* **2007**, *7*, 223–228. [[CrossRef](#)]
29. Schuster, A.; Karellas, S.; Kakaras, E.; Spliethoff, H. Energetic and economic investigation of Organic Rankine Cycle applications. *Appl. Therm. Eng.* **2009**, *29*, 1809–1817. [[CrossRef](#)]
30. Minea, V. Power generation with ORC machines using low-grade waste heat or renewable energy. *Appl. Therm. Eng.* **2014**, *69*, 143–154. [[CrossRef](#)]
31. Oyewunmi, O.A.; Markides, C.N. Thermo-Economic and Heat Transfer Optimization of Working-Fluid Mixtures in a Low-Temperature Organic Rankine Cycle System. *Energies* **2016**, *9*, 448. [[CrossRef](#)]
32. Algieri, A.; Morrone, P. Energy analysis of Organic Rankine Cycles for biomass applications. *Therm. Sci.* **2015**, *19*, 193–205. [[CrossRef](#)]
33. Mikielewicz, D.; Mikielewicz, J. A thermodynamic criterion for selection of working fluid for subcritical and supercritical domestic micro CHP. *Appl. Therm. Eng.* **2010**, *30*, 2357–2362. [[CrossRef](#)]
34. Rivera Diaz, A.; Kaya, E.; Zarrouk, S.J. ReInjection in geothermal fields—A worldwide review update. *Renew. Sustain. Energy Rev.* **2016**, *53*, 105–162. [[CrossRef](#)]
35. Algieri, A.; Morrone, P. Comparative energetic analysis of high-temperature subcritical and transcritical Organic Rankine Cycle (ORC). A biomass application in the Sibari district. *Appl. Therm. Eng.* **2012**, *36*, 236–244. [[CrossRef](#)]
36. Algieri, A.; Morrone, P. Techno-economic analysis of biomass-fired ORC systems for single-family combined heat and power (CHP) applications. *Energy Procedia* **2014**, *45*, 1285–1294. [[CrossRef](#)]
37. Algieri, A.; Morrone, P. Energetic analysis of biomass-fired ORC systems for micro-scale combined heat and power (CHP) generation. A possible application to the Italian residential sector. *Appl. Therm. Eng.* **2014**, *71*, 751–759. [[CrossRef](#)]
38. Lemmon, E.W.; Huber, M.L.; McLinden, M.O. *REFPROP Reference Fluid Thermodynamic and Transport*; NIST Online Databases; National Institute of Standards and Technology: Gaithersburg, MD, USA, 2007.
39. Liu, Q.; Duan, Y.; Yang, Z. Performance analyses of geothermal organic Rankine cycles with selected hydrocarbon working fluids. *Energy* **2013**, *63*, 123–132. [[CrossRef](#)]
40. Xi, H.; Li, M.J.; He, Y.L.; Tao, W.Q. A graphical criterion for working fluid selection and thermodynamic system comparison in waste heat recovery. *Appl. Therm. Eng.* **2015**, *89*, 772–782. [[CrossRef](#)]
41. Dai, Y.; Wang, J.; Gao, L. Parametric optimization and comparative study of Organic Rankine Cycle (ORC) for low grade waste heat recovery. *Energy Convers. Manag.* **2009**, *50*, 576–582. [[CrossRef](#)]
42. Wang, Z.Q.; Zhou, N.J.; Guo, J.; Wang, X.Y. Fluid selection and parametric optimization of organic Rankine cycle using low temperature waste heat. *Energy* **2012**, *40*, 107–115. [[CrossRef](#)]
43. Schuster, A.; Karellas, S.; Aumann, R. Efficiency optimization potential in supercritical Organic Rankine Cycles. *Energy* **2010**, *35*, 1033–1039. [[CrossRef](#)]
44. Algieri, A.; Šebo, J. Energetic Investigation of Organic Rankine Cycles (ORCs) for the Exploitation of Low-Temperature Geothermal Sources—A possible application in Slovakia. *Procedia Comput. Sci.* **2017**, *109*, 833–840. [[CrossRef](#)]
45. Li, J.; Liu, Q.; Ge, Z.; Duan, Y.; Yang, Z. Thermodynamic performance analyses and optimization of subcritical and transcritical organic Rankine cycles using R1234ze(E) for 100–200 °C heat sources. *Energy Convers. Manag.* **2017**, *149*, 140–154. [[CrossRef](#)]
46. Zhang, S.; Wang, H.; Guo, T. Performance comparison and parametric optimization of subcritical Organic Rankine Cycle (ORC) and transcritical power cycle system for low-temperature geothermal power generation. *Appl. Energy* **2011**, *88*, 2740–2754.
47. Mazzoldi, A.; Borgia, A.; Ripepe, M.; Marchetti, M.; Ulivieri, G.; della Schiava, M.; Allocca, C. Faults strengthening and seismicity induced by geothermal exploitation on a spreading volcano, Mt. Amiata, Italia. *J. Volcanol. Geotherm. Res.* **2015**, *301*, 159–168. [[CrossRef](#)]
48. Kwiatek, G.; Bohnhoff, M.; Dresen, G.; Schulze, A.; Schulte, T.; Zimmermann, G.; Huenges, E. Micro-seismicity induced during fluid-injection: A case study from the geothermal site at GrossSchönebeck, North German Basin. *Acta Geophys.* **2010**, *58*, 995–1020. [[CrossRef](#)]

49. Carlino, S.; Somma, R.; Troiano, A.; Di Giuseppe, M.G.; Troise, C.; De Natale, G. The geothermal system of Ischia Island (southern Italy): Critical review and sustainability analysis of geothermal resource for electricity generation. *Renew. Energy* **2014**, *62*, 177–196. [[CrossRef](#)]
50. Sasso, M.; Roselli, C.; Sibilio, S.; Possidente, R. Performance Assessment of Residential Cogeneration Systems in Southern Italy. Annex 42 of the International Energy Agency Energy Conservation in Buildings and Community Systems Programme. Available online: <http://www.iea-ebc.org> (accessed on 3 February 2018).
51. Shaneb, O.A.; Coates, G.; Taylor, P.C. Sizing of residential μ CHP systems. *Energy Build.* **2011**, *43*, 1991–2001. [[CrossRef](#)]



© 2018 by the author. Licensee MDPI, Basel, Switzerland. This article is an open access article distributed under the terms and conditions of the Creative Commons Attribution (CC BY) license (<http://creativecommons.org/licenses/by/4.0/>).